Core-level photoelectron spectroscopy study of interface structure of hydrogen-intercalated graphene on *n*-type 4*H*-SiC(0001)

Fumihiko Maeda,[1] Shinichi Tanabe,[1] Shingo Isobe,[1,2,*] and Hiroki Hibino[1]

[1]*NTT Basic Research Laboratories, Nippon Telegraph and Telephone co., 3-1 Morinosato-Wakamiya, Atsugi-shi, Kanagawa 243-0198, Japan*
[2]*Department of Mechanical Engineering, Nagaoka University of Technology, 1603-1 Kamitomioka, Nagaoka, Niigata 940-2188 Japan*

The interface structure of hydrogen-intercalated graphene/SiC(0001), formed by annealing SiC substrates with the buffer layer at high temperature under atmospheric molecular hydrogen, was investigated by core-level photoelectron spectroscopy. The investigation of C 1s spectra, captured before and after the annealing at various temperatures in a vacuum, indicates that residual materials (hydrocarbon and hydrogen) stayed at the interface on the as-treated sample and remained there until annealing at around 700 °C. These residual materials would cause distortion of the graphene. The analysis of Si 2p photoelectron spectra reveals insufficient termination of Si-dangling bonds at the interface by hydrogen and that significant interface states remained. The interface states of Si dangling bonds are plausible origins of Fermi level pinning and would act as charged impurities. These distortion and charged impurities should degrade the electronic performance of graphene in this system.

I. INTRODUCTION

Large-scale integration is crucial for the application of graphene for future electric and photonic devices. For this purpose, wafer-scale graphene is required and several methods, which are based on familiar phenomena[1–3] in the surface science field, have been proposed. A particularly promising method for wafer-scale graphene formation is atmospheric pressure graphitization of silicon carbide (SiC)[4] because it allows us to directly form high-quality graphene on an insulating substrate without a transfer process. However, the substrate, including the $6\sqrt{3} \times 6\sqrt{3}$ reconstructed interface layer (the so-called "buffer layer"), induces strong electron–phonon coupling, resulting in the considerable reduction of mobility as the temperature is increased from the cryogenic temperature.[5]

Meanwhile, a quasi-free-standing (QFS) state of epitaxial graphene has been achieved by breaking bonds between the C atoms of buffer layer and Si atoms of the SiC substrate below the buffer layer and by terminating Si-dangling bonds at the interface by hydrogen.[6,7] Consequently, hydrogen is intercalated between the graphene and SiC substrate. Hence, in this paper, QFS graphene hereafter refers to the hydrogen-intercalated graphene on SiC. Because of the decoupling of the buffer layer from its substrate, this method was expected to suppress the aforementioned mobility reduction in the graphene and to achieve comparable performance with that of the real suspended graphene.[8] However, the expected performance has not been reached[9,10] because of Coulomb scattering caused by charged impurities.[11] The origin of the charged impurities may be the interface. However, the detailed interface structure has not yet been revealed.

In Refs. 9–11, QFS graphene was formed from the buffer layer on SiC(0001) by annealing it in molecular hydrogen at atmospheric pressures, which is a simple method, basically the same as in Ref. 6. Although the formation of Si-H bonds at the interface was observed, it was not confirmed whether this simple method provides complete termination. Therefore, we studied the interface structure of

hydrogen-intercalated graphene on SiC(0001) by investigating core-level photoelectron spectra in detail through the annealing process in a vacuum.

II. EXPERIMENTAL

We used *n*-type 4*H*-SiC(0001) substrates, on which the QFS monolayer (ML) and bilayer (BL) graphene were formed by hydrogen intercalation. For the QFS ML graphene, first the SiC substrates were annealed at 1250 °C in H_2 ambient of 25 Torr to clean the surface and were subsequently annealed at 1650 °C in Ar ambient at 600 Torr to form the buffer layer in the infrared high-temperature annealing system. Then, the sample was annealed at 800 °C in an atmospheric H_2 ambient for the hydrogen intercalation. The QFS BL graphene was prepared by the hydrogen intercalation of the epitaxial ML graphene on the SiC(0001) with the buffer layer, which was formed by annealing at 1650 °C in Ar ambient at 100 Torr. In this case, the sample was heated to 1000 °C in an atmospheric H_2 ambient for the hydrogen intercalation.

After the hydrogen intercalation, the substrates were set in an x-ray photoelectron spectroscopy (XPS) measurement system equipped with a monochromatized Al Kα source (1486.6 eV) and a photoelectron analyzer. In this XPS system, whose base pressure is less than 1.0×10^{-9} Torr, the substrates were annealed for 10 min from 250 to 750 °C in increments of 100 °C and, after annealing at each elevated temperature, photoelectrons were measured *in situ* after the substrates had been cooled down to less than 100 °C. The takeoff angle of the photoelectrons was set at 25° from the surface so that the measurements were performed under the surface-sensitive condition. A molecular beam epitaxy (MBE) growth system,[12] whose base pressure is less than 5.0×10^{-10} Torr, is connected to the XPS system. The sample was transferred to the MBE system for the annealing from 850 to 965 °C and then transferred back to the XPS system via ultrahigh vacuum without exposure to air to measure photoelectron spectra. To calibrate binding energy, Fermi-edge spectra were measured on a gold plate, and the total energy
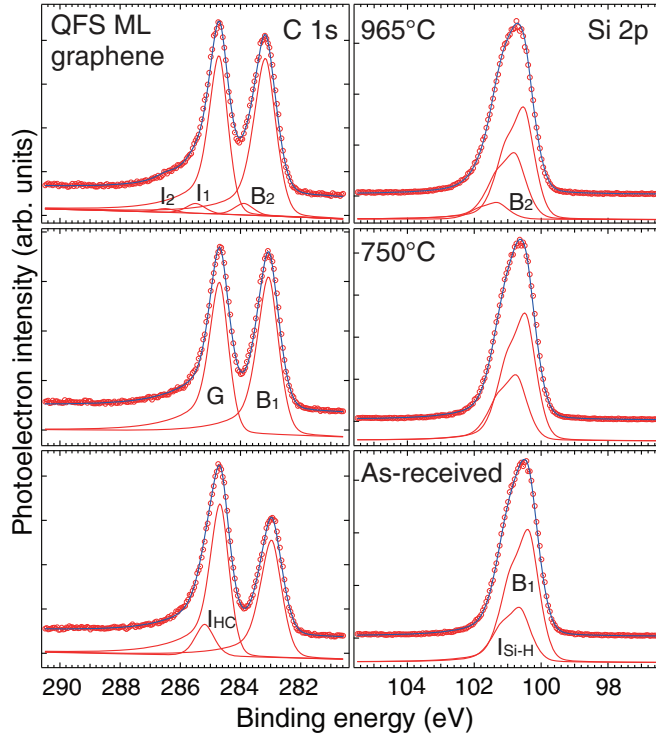
FIG. 1. (Color online) Typical C 1s (left) and Si 2p (right) core-level photoelectron spectra captured from the as-received and annealed samples for the QFS ML graphene on hydrogen-terminated SiC(0001). Circles are experimental data, and lines indicate fitting results. In C 1s spectra, the components are attributed, respectively, to bulk SiC of hydrogen-terminated SiC (B_1), the buffer layer (B_2), graphite/graphene (G), and the two interface states of the buffer layer (I_1 and I_2). The component of hydrocarbon is denoted I_{HC}. In Si 2p spectra, B_1 and B_2 are components corresponding, respectively, to the same C 1s. Component I_{Si-H} corresponds to a hydrogen-Si bond at the interface.

resolution of photoelectron measurements was estimated to be 0.5 eV.

III. RESULTS AND DISCUSSION

A. QFS ML Graphene

Figure 1 shows typical core-level photoelectron spectra of C 1s and Si 2p, captured before (as-received) and after annealing of the QFS ML graphene at $750\,°C$ and $965\,°C$. For these spectra, a peak-fit procedure was performed, and the results are represented by lines. In the Si 2p spectra of the as-received sample and after annealing at $750\,°C$, only two peaks are resolved, and they are attributed to SiC-bulk (B_1) and Si-H bonding states (I_{Si-H}), which were also observed in a previous study.[6] They indicate that the Si atoms at the surface of SiC are terminated by hydrogen. Deriving peak intensities from the areas of these two peaks and using the formula described in Ref. 13 with $\lambda_1 = 13$ Å[14] for the electron mean-free path and $A = 1$, which indicates that the density of Si atoms for Si-H bonds is identical to that of the SiC-bulk, we determined the coverage of the Si-H bonds before the annealing to be about 0.79 MLs. This suggests that a considerable number
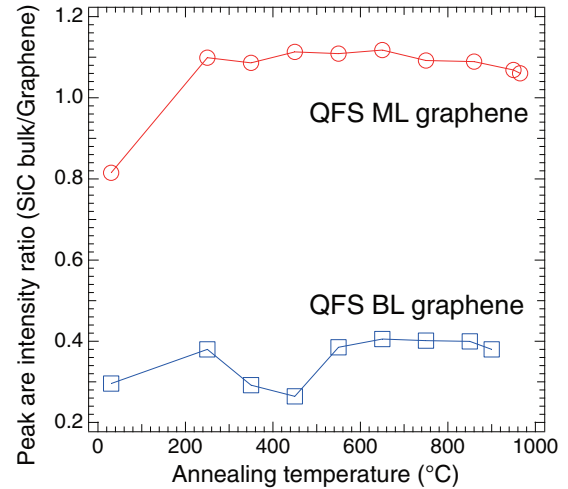

FIG. 2. (Color online) Summary of intensity ratios of peak areas in C 1s spectra versus annealing temperature for QFS ML (circles) and BL (squares) graphene on hydrogen-terminated SiC(0001).

of Si-dangling bonds still remain at the interface below the graphene.

In the C 1s spectra, two major peaks (graphene and SiC-bulk) are observed in all spectra, and a small peak component (hydrocarbon[15]) is resolved in the spectrum of the as-received sample before annealing. This small peak, obtained for the first time by the precise deconvolution of the C 1s spectra before and after annealing at several steps, indicates that hydrocarbon remained at the interface but disappeared after annealing at $750\,°C$. Furthermore, the intensity ratio of the peak areas of the SiC bulk to that of the graphene was smaller than unity before the annealing, whereas that after the annealing at $750\,°C$ was more than unity. If species adsorbed on the graphene surface had simply desorbed because of the annealing, the intensity ratio would not change. Consequently, this change in the intensity ratio indicates that unidentified species remained at the interface between the QFS ML graphene and the SiC bulk before the annealing, and these species disappeared (probably desorbed) afterward.

The intensity ratios of peak areas in the C 1s spectra versus annealing temperature are summarized in Fig. 2. The ratio increased after $250\,°C$ annealing and remained approximately constant until annealing at $850\,°C$. This increase corresponds to the desorption of unidentified species from the interface. Meanwhile, the decrease in the ratio for annealing above $850\,°C$ corresponds to the appearance of the peak component of the buffer layer[6] in Si 2p (B_2) and C 1s (B_2, I_1, and I_2) and indicates that the ML graphene on the hydrogen-terminated SiC started to transform into a buffer layer and that its domain area became a certain size.

Next, we discuss the possible origin of the undefined species. In a XPS spectrum ranging in binding energy from 0 to 1350 eV (not shown here), large graphene- and SiC-related photoelectrons and Auger peaks were observed, while a faint photoelectron peak of O 1s and Auger peak of O KLL were observed before the annealing, which disappeared after annealing at $250\,°C$. Since the XPS measurement cannot directly determine whether hydrogen exists or not, the unidentified species could also be hydrogen-related materials. From the
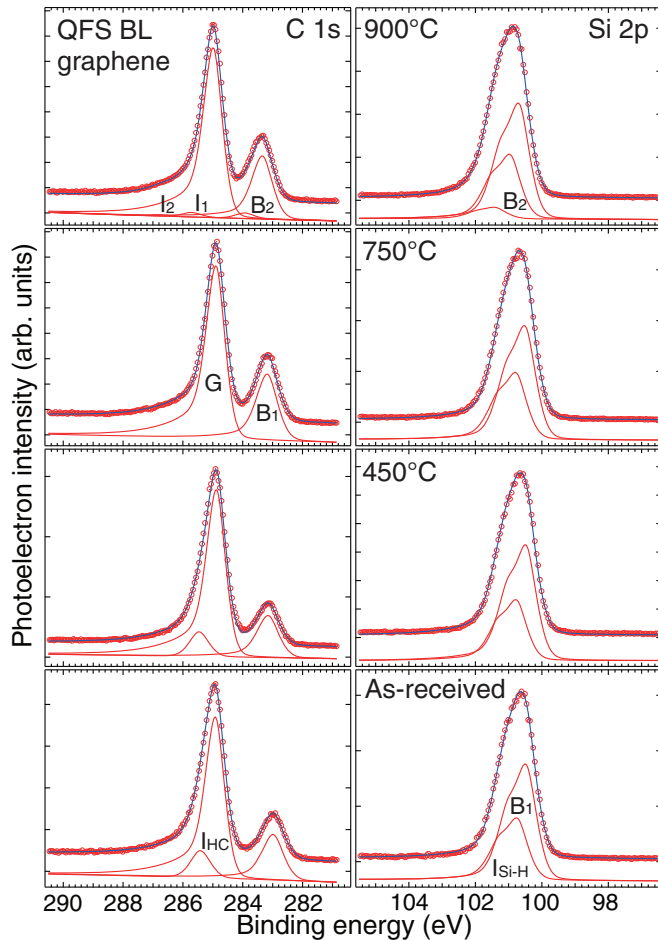
FIG. 3. (Color online) Typical C 1s and Si 2p core-level photo-electron spectra captured from the as-received and annealed samples for the QFS BL graphene on the hydrogen terminated SiC(0001).

photoelectron intensity attenuation of Si 2p, we estimated the thickness of the unidentified species to be nominally about 2.0 Å, which corresponds to 0.6 MLs of graphene. However, the peak intensity of the O 1s corresponds to 0.02 MLs, if the graphene is assumed to be 1 ML in this sample, and is negligibly small. Therefore, we presume that the possible species is hydrocarbon from XPS spectra. However, carbon atoms in the hydrocarbon are estimated to be 0.17 MLs using the ratio of the component peak-area intensity of hydrocarbon and graphene, which is too small to account for the amount of the undefined species even if hydrogen atoms bonded to these carbon atoms. Therefore, hydrogen molecules could also be the undefined species because hydrogen is virtually impossible to detect by XPS.

B. QFS BL Graphene

We performed a similar experiment for QFS BL graphene prepared by the hydrogen intercalation of the epitaxial ML graphene on the SiC(0001) with the buffer layer. Figure 3 shows the typical spectra of C 1s and Si 2p before and after annealing under ultrahigh vacuum. A similar change as in the QFS ML graphene was observed, and a hydrocarbon component was also resolved in the C 1s spectra before annealing, although it was observed after annealing at 450 °C.

This hydrocarbon component disappeared after annealing at 650 °C in this case. Furthermore, the intensity ratios of the SiC bulk to the graphene peaks in the C 1s are smaller than those in the QFS ML graphene. Because, in this case, QFS graphene is one layer thicker than the QFS ML graphene, the graphene peak intensities are nearly two times larger, and the photoelectron attenuation by the thicker overlayer causes the decrease in the SiC-bulk peak intensities. These result in the smaller intensity ratios and are consistent with BL.

In addition, when looking at the Si 2p, the intensity ratios of the Si-H bonding to the SiC bulk both before and after annealing are slightly larger than those of the QFS ML graphene. Using the intensity ratio of these two peaks, we estimated the coverage of Si-H bonds at room temperature to be 0.97 MLs, suggesting that the Si-dangling bonds at the interface remained, although Si at the interface was considerably terminated by hydrogen.

In the QFS ML graphene, the coverage was 0.79 MLs, as mentioned above, indicating that the hydrogenation of the Si at the interface is further insufficient. We think that this difference in the coverage of hydrogenated Si at the interface between the QFS BL and ML graphene was caused by difference in hydrogenation temperatures: In the case of the QFS BL graphene, the annealing temperature was 1000 °C, while that of the QFS ML graphene was 800 °C. The lower annealing temperature in the QFS ML graphene may lower the cracking efficiency of hydrogen molecule and reduce the reaction of hydrogen with Si atoms at the interface. In addition, the transmission efficiency of hydrogen through graphene would also be lower at the low temperature. Since we are afraid of the degradation in the QFS ML graphene by higher tempera-ture annealing, we set the temperature of the QFS ML graphene to lower than that of QFS BL graphene. Consequently, the coverage of hydrogenated Si should be smaller in the QFS ML graphene. Hence, the hydrogen-intercalation condition has to be optimized for the complete termination of Si-dangling bonds, while there is more room for improvement for the case of the QFS ML graphene.

The intensity ratios of peak areas in the C 1s spectra versus annealing temperature are also summarized in Fig. 2. This change is similar to that of the QFS ML graphene in which the intensity ratios increase after annealing at 250 °C and remain approximately constant at high temperatures until annealing at 850 °C. However, the exception is the annealing temperatures of 350 and 450 °C: there is a trough whose values are smaller than the initial value. These results indicate that the aforementioned unidentified species once desorbed from the interface after annealing at 250 °C but reappeared at the interface at the annealing temperature of around 400 °C and finally disappeared at 650 °C.

Since the peak of the hydrocarbon appeared with similar peak height of the two temperatures, the interface structures were identical to those of the as-received sample. However, when the sample was annealed at 350 and 450 °C, because the vacuum was less than 10^{-8} Torr, it would be impossible for hydrocarbons or hydrogen to be incorporated into the interface between graphene and SiC if they were supplied from the vacuum environment. Consequently, the only possible source is the substrate. Since the diffusion of hydrocarbon gas in SiC is unlikely to happen, we think that the gas would be supplied
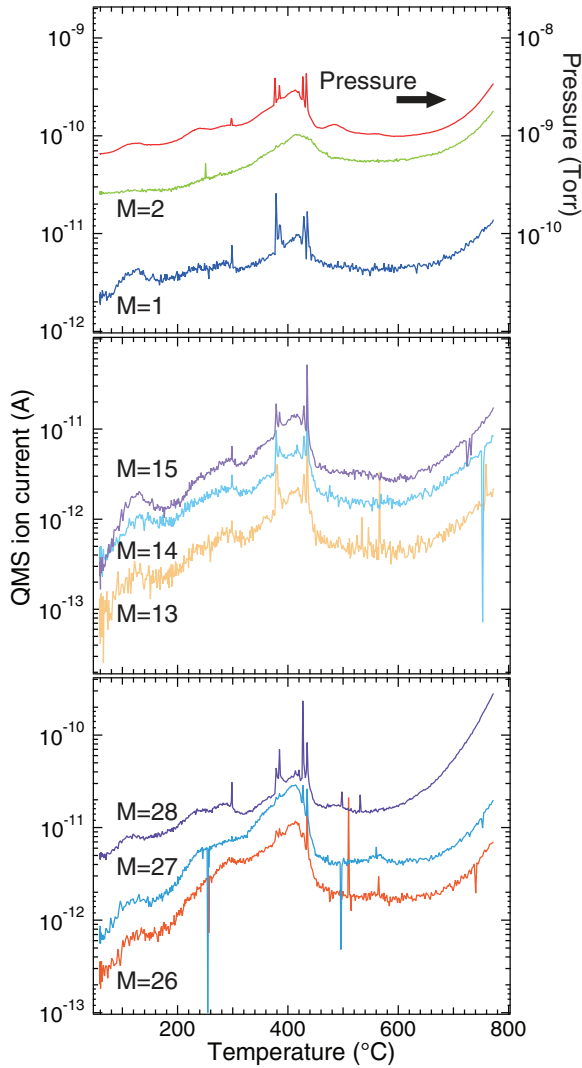
FIG. 4. (Color online) Spectra of ions with several masses measured from the QFS BL graphene on the SiC by thermal desorption spectroscopy. Masses 1 and 2 are related to hydrogen and the other masses ($M = 13$–15, 25–28) correspond to the fragment ions dissociated from C_2 hydrocarbons. Top spectrum is for the environmental pressure.

from the other face (sides and back) of the substrate and then diffuse to the surface through the interface between the graphene layers and SiC. This is a plausible pathway because the graphene formed on the other sides of the SiC substrate is much thicker than that on the (0001)-face. Regarding hydrogen, theoretical studies predict that its ion (proton) is highly mobile at room temperature[16] and can diffuse through the channel of an interstitial site.[17] Further, its molecule is stable and freely mobile.[16,18] Thus, hydrogen will diffuse through SiC bulk, although the form (ion, atomic, or molecule) during the diffusion is not clear.

To verify the above interpretation, we estimated the amount of desorbed molecules by measuring their ion currents with selecting the masses using a quadrupole mass spectrometer with increasing sample temperature [thermal desorption spectroscopy (TDS)]. Figure 4 shows the TDS spectra of the ions with several masses, which were released from the sample of

the QFS BL graphene. The masses of 1 and 2 ($M = 1, 2$) are related to hydrogen and the other masses ($M = 13$–15, 25–28) correspond to the fragment ions dissociated from C_2 hydrocarbons.[19,20] These spectra indicate that hydrogen and hydrocarbon indeed desorb. Particularly, the peaks at 400 °C indicate that the hydrogen and hydrocarbon were intensely supplied from the substrate and that they desorbed from the surface. In this case, when heating was suspended, the gases stopped to desorb. Some amount of them remained at the interface of the graphene and SiC because the BL may have been sufficiently thick to confine the gases there, whereas the gases were almost completely released for the QFS ML graphene in this temperature range. This is consistent with the trough at 400 °C for the QFS BL graphene in Fig. 2. Therefore, these TDS results support our interpretations of the accumulation of the gases at the interface and the change in the ratio of C 1s peak intensities.

Meanwhile, this result indicates that hydrogen diffusion through SiC bulk is easier than that through graphene. This trend is consistent with theoretical calculation of the diffusion barriers of atomic hydrogen: 1.0 eV for the c channel [the c channel is in the (0001) direction of SiC],[16] 2.55 eV for the QFS ML graphene,[21] and 3.73 eV for the graphene without stretching.[21] Since the form during the diffusion is not clear at present, this is not direct evidence; however, we can presume the ease of diffusion for each case from these values. In the case of the QFS BL graphene, the top-layer of graphene slightly relaxes, and stretching is smaller than the QFS ML graphene. This would result in a larger diffusion barrier for the QFS BL graphene because the value becomes closer to that without stretching. We speculate that this larger diffusion barrier caused the difference in the temperature dependences of remaining species at the interface, which were observed as the intensity ratios of C 1s in Fig. 2.

C. Band-bending and dangling bond at the interface

The Fermi level at the surface of semiconductors often differs from that of the bulk. This is caused by electron occupation of surface states and charge transfer from the bulk, which results in band bending. The band bending induces a shift of electrical potential at the surface from the bulk and can be observed as the core-level shift of photoelectrons.

Thus, using the bulk peak position of Si 2p core level in a different situation for this material, the value of the band-bending and pinning position can be calculated when the bulk-peak position of a core level is obtained. For instance, the schematic diagram of the surface band structure of the $\sqrt{3} \times \sqrt{3}$-reconstructed n-type $4H$-SiC(0001) is illustrated in Fig. 5(a). In this case, the surface band shifts upward by 0.65 eV[22] from the bulk. When we use the band gap of 3.25 eV[23] and the Fermi-level position below the conduction band minimum of 0.1 eV,[15,24] which is the value for n-type $6H$-SiC and would be almost identical to that for $4H$-SiC because ionization energy of the donor level is similar,[25] the pinning position of the Fermi level can be calculated to be 2.5 eV above the valence band maximum (VBM) using this energy diagram. In addition, the peak position of the bulk component of Si 2p, 101.0 eV[22,26] in this case, includes the upward shift of the band bending.
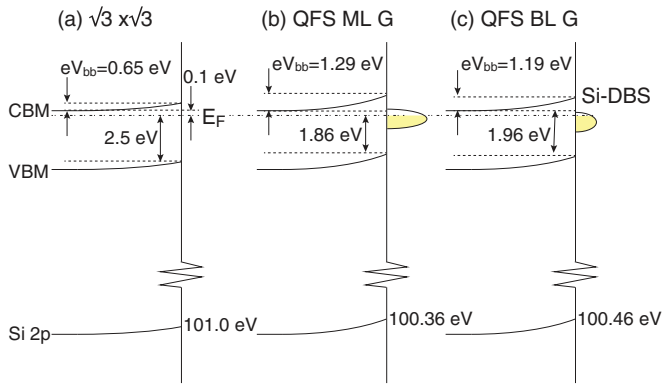
FIG. 5. (Color online) Schematic diagram of surface band structures including Si 2p of (a) $\sqrt{3} \times \sqrt{3}$ reconstructed $4H$-SiC (0001), (b) QFS ML, and (c) BL graphene on hydrogen-terminated $4H$-SiC(0001). Values of Si 2p in (b) and (c) are experimental results; the others are calculated on the basis of those in (a) described in the references.

FIG. 6. (Color online) Interface structure model of QFS graphene on SiC(0001) formed by hydrogen intercalation in the present condition.

Figure 5(b) shows the energy diagram for the QFS ML graphene. In the as-received sample, the bulk peak of Si 2p is at 100.36 eV, which is obtained from the bottom-right panel of Fig. 1. From the difference between the values of the $\sqrt{3}$ and the QFS ML graphene, the values of the band-bending and Fermi level position above the VBM are, respectively, calculated to be 1.29 and 1.86 eV. When the bulk peak position in the bottom-right panel of Fig. 3 is used, by using the same procedure, the values for the QFS BL graphene are 1.19 and 1.96 eV. This relationship between these values is illustrated in Fig. 5(c).

Because these band-bending values are very large and far from the condition in the flat band, our results regarding the Fermi-level position, estimated by the Si 2p photoelectron measurement, indicate that the surface Fermi level is pinned to the significantly large interface states in the QFS ML and BL graphene of this study. From the estimation of hydrogen coverage at the interface using the Si-H component in the Si 2p core-level photoelectron spectra, it is clear that a considerable number of Si atoms at the interface are terminated by hydrogen. However, we found that the hydrogen coverage estimated using the intensity ratios between the components of Si-H and SiC-bulk are less than unity. Therefore, for the interface states, the Si-dangling bond is the most probable origin. In addition, a theoretical investigation for the $4H$-SiC(0001) predicts that the dangling-bond state of Si is located 1.8 eV above the VBM,[27] which is smaller but close to the aforementioned values. If we assume the distribution of the interface states and their occupation by electrons, as in the illustrations in Fig. 5(b) and (c), our result is consistent with the theoretical study. Thus, the estimation of the pinning position using core-level shifts supports the interpretation that hydrogen termination is not sufficient and that a high density of Si dangling bonds remains at the interface. This is in agreement with the interpretation that Si-dangling bonds act as charged impurities, and the QFS ML graphene mobility is reduced by Coulomb scattering.[11]

Meanwhile, when the density of interface states is very large, our result indicates that the core-level position considerably shif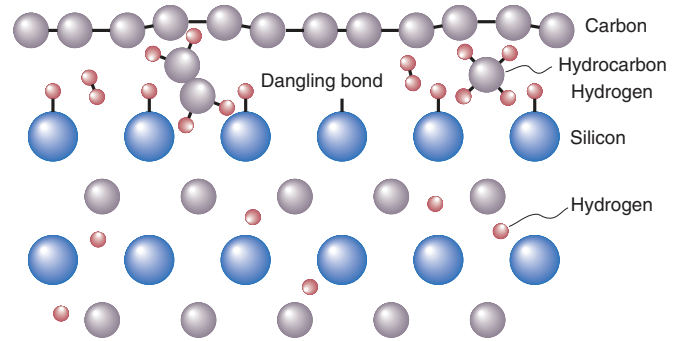ts upward in the n-type SiC, indicating that the core-level shift of the bulk peak is a good index for evaluating charge impurities at the interface. If we can optimize the hydrogenation condition and completely eliminate the interface states, we believe that a flat band will be achieved because, on bare SiC(0001) without the graphene formation, a flat band has already been realized by hydrogenation of the surface, which was evaluated by core-level photoelectron spectroscopy.[15] Therefore, for such optimization of the hydrogenation condition in the QFS graphene on SiC, the core-level shift would be a useful index.

D. Interface structure

Through the above discussions, certain aspects of the interface structure of the QFS graphene on SiC(0001) is clarified. The changes in the peak intensity ratios of the QFS graphene and SiC bulk in the C 1s spectra revealed that there are unidentified materials at the interface in the as-received sample. Then, the fitting of the C 1s spectra revealed that hydrocarbon is one of the possible unidentified materials. Furthermore, the other elements related to graphene, SiC-bulk, and hydrocarbon were not detected by the photoelectron spectroscopy, suggesting that the rest of the material, which satisfies the change in the intensity ratio, would be hydrogen. Meanwhile, the investigation of the band bending using a Si 2p core level revealed that a significant number of the Si-dangling bond remain at the interface. These results are summarized in the illustration in Fig. 6.

Considering this interface structure, the distribution of residual materials at the interface results in the distribution of the distance between the QFS graphene and SiC bulk. This would induce distortion in the QFS graphene and thereby cause the reduction of the mobility. Hence, this residual material is also an important factor affecting the mobility.[28] Therefore, our present work suggests that both the complete termination of Si-dangling bonds and removal of residue at the interface are the keys to realizing the intrinsic mobility of QFS graphene.

IV. CONCLUSIONS

We studied the interface structure of hydrogen-intercalated graphene on n-type $4H$-SiC(0001) by core-level photoelectron spectra through the annealing process in a vacuum. Our results indicate that termination of Si-dangling bonds at the interface by hydrogen is not sufficient, and significant interface states

remain when hydrogen is intercalated by simple annealing at high temperature from 800 to 1000 °C in a hydrogen ambient of atmospheric molecular hydrogen. The estimation of the pinning position of the Fermi level suggests that a plausible origin of the interface states is the large number of Si-dangling bonds at the interface, which act as charged impurities to reduce the QFS graphene mobility. Meanwhile, the investigation of C 1s core-level spectra indicated that residual materials at the interface remain on the as-treated and low-temperature-annealed samples. Furthermore, it was revealed that one of the residual materials is hydrocarbon and

that hydrogen is also a possible one. These results suggest that both the complete termination of Si-dangling bonds and removal of residues at the interface are the keys to improving the electronic performance of QFS graphene on SiC(0001) formed by hydrogen intercalation.

---

*This research was performed while S. Isobe was at NTT Basic Research Laboratories during his stay as a trainee.

[1] A. J. van Bommel, J. E. Crombeen, and A. van Tooren, Surf. Sci. **48**, 463 (1975).

[2] C. Oshima and A. Nagashima, J. Phys.: Condens. Matter **9**, 1 (1997).

[3] L. C. Isett and J. M. Blakely, Surf. Sci. **58**, 397 (1976).

[4] K. V. Emtsev, A. Bostwick, K. Horn, J. Jobst, G. L. Kellogg, L. Ley, J. L. McChesney, T. Ohta, S. A. Reshanov, J. Rohrl, E. Rotenberg, A. K. Schmid, D. Waldmann, H. B. Weber, and T. Seyller, Nat. Mater. **8**, 203 (2009).

[5] S. Tanabe, Y. Sekine, H. Kageshima, M. Nagase, and H. Hibino, Phys. Rev. B **84**, 115458 (2011).

[6] C. Riedl, C. Coletti, T. Iwasaki, A. A. Zakharov, and U. Starke, Phys. Rev. Lett. **103**, 246804 (2009).

[7] C. Virojanadara, A. A. Zakharov, R. Yakimova, and L. I. Johansson, Surface Sci. **604**, L4 (2010).

[8] X. Du, I. Skachko, A. Barker, and E. A. Andrei, Nat. Nanotechnol. **3**, 491 (2008).

[9] F. Speck, J. Jobst, F. Fromm, M. Ostler, D. Waldmann, M. Hundhausen, H. B. Weber, and T. Seyller, Appl. Phys. Lett. **99**, 122106 (2011).

[10] D. Waldmann, J. Jobst, F. Speck, T. Seyller, M. Krieger, and H. B. Weber, Nat. Mater. **10**, 357 (2011).

[11] S. Tanabe, M. Takamura, Y. Harada, H. Kageshima, and H. Hibino, App. Phys. Expr. **5**, 125101 (2012).

[12] F. Maeda and H. Hibino, Diamond & Related Materials **34**, 84 (2013).

[13] F. Maeda, H. Hibino, I. Hirosawa, and Y. Watanabe, e-J. Surf. Sci. Nanotech. **9**, 58 (2011).

[14] N. Sieber, Th. Seyller, L. Ley, D. James, J. D. Riley, R. C. G. Leckey, and M. Polcik, Phys. Rev. B **67**, 205304 (2003).

[15] Th. Seyller, J. Phys.: Condens. Matter **16**, S1755 (2004).

[16] M. Kaukonen, C. J. Fall, and J. Lento, Appl. Phys. Lett. **83**, 923 (2003).

[17] B. Aradi, A. Gali, P. Deák, J. E. Lowther, N. T. Son, E. Janzén, and W. J. Choyke, Phys. Rev. B **63**, 245202 (2001).

[18] B. Aradi, P. Deák, A. Gali, N. T. Son, and E. Janzén, Phys. Rev. B **69**, 233202 (2004).

[19] P. Kusch, A. Hustrulid, and J. T. Tate, Phys. Rev. **52**, 843 (1937).

[20] J. A. Hipple, Jr., Phys. Rev. **53**, 530 (1938).

[21] A. Markevich, R. Jones, S. Öberg, M. J. Rayson, J. P. Goss, and P. R. Briddon, Phys. Rev. B **86**, 045453 (2012).

[22] C. Virojanadara, P.-A. Glans, T. Balasubramanian, L. I. Johansson, E. B. Macak, Q. Wahab, and L. D. Madsen, J. Electron. Mater. **31**, 1353 (2002).

[23] F. Ren and J. C. Zolper, *Wide Energy Bandgap Electronic Devices* (World Scientific Publishing Co. Pte. Ltd., 5 Toh Tuck Link, Singapore, 2003), p. 344.

[24] Th. Seyller, K. V. Emtsev, K. Gao, F. Speck, L. Ley, A. Tadich, L. Broekman, J. D. Riley, R. C. G. Leckey, O. Rader, A. Varykhalov, and A. M. Shikin, Surf. Sci. **600**, 3906 (2006).

[25] M. Ikeda, H. Matsunami, and T. Tanaka, Phys. Rev. B **22**, 2842 (1980).

[26] L. I. Johansson, F. Owman, and P. Mårtensson, Surf. Sci. **360**, L483 (1996).

[27] T. Ohnuma, H. Tsuchida, and T. Jikimoto, Materials Science Forum **457–460**, 1297 (2004).

[28] M. I. Katsnelson and A. K. Geim, Philos. Trans. R. Soc. A **366**, 195 (2008).